

# $[\text{Mn}_2^{\text{III}}(\text{5-Rsaltmen})_2\text{Ni}^{\text{II}}(\text{pao})_2(\text{L})]^{2+}$ : An $S_{\text{T}}=3$ Building Block for a Single-Chain Magnet That Behaves as a Single-Molecule Magnet

Hitoshi Miyasaka,<sup>\*,[a]</sup> Tomohiro Nezu,<sup>[a]</sup> Kuniyoshi Sugimoto,<sup>[c]</sup> Ken-ichi Sugiura,<sup>[a]</sup> Masahiro Yamashita,<sup>[a, b]</sup> and Rodolphe Clérac<sup>\*,[d]</sup>

**Abstract:**  $\text{Mn}^{\text{III}}\text{-Ni}^{\text{II}}\text{-Mn}^{\text{III}}$  linear-type trinuclear complexes bridged by oximate groups were selectively synthesized by the assembly reaction of  $[\text{Mn}_2(\text{5-Rsaltmen})_2(\text{H}_2\text{O})_2](\text{ClO}_4)_2$  (5-Rsaltmen<sup>2-</sup> = *N,N'*-(1,1,2,2-tetramethylethylene) bis(5-R-salicylideneimine); R = Cl, Br) with  $[\text{Ni}(\text{pao})_2(\text{phen})]$  (pao<sup>-</sup> = pyridine-2-aldoximate; phen = 1,10-phenanthroline) in methanol/water:  $[\text{Mn}_2(\text{5-Rsaltmen})_2\text{Ni}(\text{pao})_2(\text{phen})](\text{ClO}_4)_2$  (R = Cl, **1**; R = Br, **2**). Structural analysis revealed that the  $[\text{Mn}^{\text{III}}\text{-ON-Ni}^{\text{II}}\text{-NO-Mn}^{\text{III}}]$  skeleton of these trimers is in every respect similar to the repeating unit found in the previously reported series of 1D materials  $[\text{Mn}_2(\text{saltmen})_2\text{Ni}(\text{pao})_2(\text{L}^1)_2](\text{A})_2$  ( $\text{L}^1$  = pyridine, 4-picoline, 4-*tert*-butylpyridine, *N*-methylimidazole; A =  $\text{ClO}_4^-$ ,  $\text{BF}_4^-$ ,  $\text{PF}_6^-$ ,  $\text{ReO}_4^-$ ). Recently, these

1D compounds have attracted a great deal of attention for their magnetic properties, since they exhibit slow relaxation of the magnetization (also called single-chain magnet (SCM) behavior). This unique magnetic behavior was explained in the framework of Glauber's theory, generalized for chains of ferromagnetically coupled anisotropic spins. Thus, in these 1D compounds, the  $[\text{Mn}^{\text{III}}\text{-ON-Ni}^{\text{II}}\text{-NO-Mn}^{\text{III}}]$  unit was considered as an  $S_{\text{T}}=3$  anisotropic spin. Direct-current magnetic measurements on **1** and **2** confirm their  $S_{\text{T}}=3$  ground state and strong

uniaxial anisotropy ( $D/k_{\text{B}} \approx -2.4$  K), in excellent agreement with the magnetic characteristic deduced in the study on the SCM series. The ac magnetic susceptibility of these trimers is strongly frequency-dependent and characteristic of single-molecule magnet (SMM) behavior. The relaxation time  $\tau$  shows a thermally activated (Arrhenius) behavior with  $\tau_0 \approx 1 \times 10^{-7}$  s and  $\Delta_{\text{eff}}/k_{\text{B}} \approx 18$  K. The effective energy barrier for reversal of the magnetization  $\Delta_{\text{eff}}$  is consistent with the theoretical value (21 K) estimated from  $|D|S_{\text{T}}^2$ . The present results reinforce consistently the interpretation of the SCM behavior observed in the  $[\text{Mn}_2(\text{saltmen})_2\text{Ni}(\text{pao})_2(\text{L}^1)_2](\text{A})_2$  series and opens new perspectives to design single-chain magnets.

**Keywords:** heterometallic complexes • magnetic properties • single-chain magnets • single-molecule magnets

## Introduction

An active research domain in the field of molecule-based magnetism is devoted to the design of new molecular or


one-dimensional (1D) systems exhibiting slow relaxation of their magnetization. This type of behavior was first observed in molecular clusters often called single-molecule magnets (SMMs).<sup>[1]</sup> Since the discovery of SMM behavior in the

[a] Dr. H. Miyasaka, T. Nezu, Prof. K.-i. Sugiura, Prof. M. Yamashita  
Department of Chemistry, Graduate School of Science  
Tokyo Metropolitan University  
1-1 Minami-Ohsawa, Hachioji, Tokyo 192-0397 (Japan)  
"Structural Ordering and Physical Properties"  
PRESTO, Japan Science and Technology Agency (JST)  
4-1-8 Honcho Kawaguchi, Saitama 332-0012 (Japan)  
Fax: (+81)426-77-2525  
E-mail: miyasaka@comp.metro-u.ac.jp

[b] Prof. M. Yamashita  
Current address: Department of Chemistry, Graduate School  
of Science  
Tohoku University, Aramaki-Aza-Aoba, Aoba-ku, Sendai 980-8578  
(Japan)  
CREST, JST, 4-1-8 Honcho Kawaguchi, Saitama 332-0012 (Japan)

[c] Dr. K. Sugimoto  
X-ray Research Laboratory, Rigaku Co., Ltd.  
3-9-12 Matsubara-cho, Akishima, Tokyo 196-8666 (Japan)

[d] Dr. R. Clérac  
Centre de Recherche Paul Pascal, CNRS UPR 8641  
115 avenue du Dr. A. Schweitzer, 33600 Pessac (France)  
Fax: (+33)556-845-600  
E-mail: clerac@crpp-bordeaux.cnrs.fr

 Supporting information for this article is available on the WWW under <http://www.chemeurj.org/> or from the author.

mixed-valent  $\text{Mn}_{12}^{\text{III/IV}}$  cluster  $[\text{Mn}_{12}\text{O}_6(\text{O}_2\text{CCH}_3)_{12}(\text{H}_2\text{O})_4]$ ,<sup>[2]</sup> a large number of transition-metal-based SMM clusters have been reported.<sup>[3–9]</sup> In these materials, the slow relaxation of the magnetization is induced by individual molecules and the combined effect of their uniaxial anisotropy ( $D$ ) and high-spin ground state ( $S_T$ ). These two characteristics create an energy barrier ( $\Delta = |D|S_T^2$  for integer spin and  $\Delta = |D|(S_T^2 - 1/4)$  for half-integer spin) between the two thermodynamically equivalent spin configurations  $\pm m_s$ , that is, between spin-up and spin-down states. Therefore, below a characteristic temperature called the blocking temperature  $T_B$ , the thermal energy is no longer able to overcome the energy barrier and allow the spin to explore the two configurations. Thereby, the spin is trapped or “frozen” in one of the two equivalent potentials. This molecular property can be observed at the bulk level when a magnetic field is applied at which the magnetization of the material saturates below  $T_B$ . Thus the relaxation time of the magnetization  $\tau$  can be measured as a function of temperature by using the direct time dependence of the magnetization or the frequency dependence of the ac susceptibility. It exhibits thermally activated behavior [Arrhenius law, Eq. (1)], where  $\tau_0$  is a pre-exponential factor characteristic of the molecular system,  $\Delta_{\text{eff}}$  the effective energy barrier (equal to  $\Delta$  when quantum tunneling of the magnetization is not efficient), and  $k_B$  the Boltzmann constant.

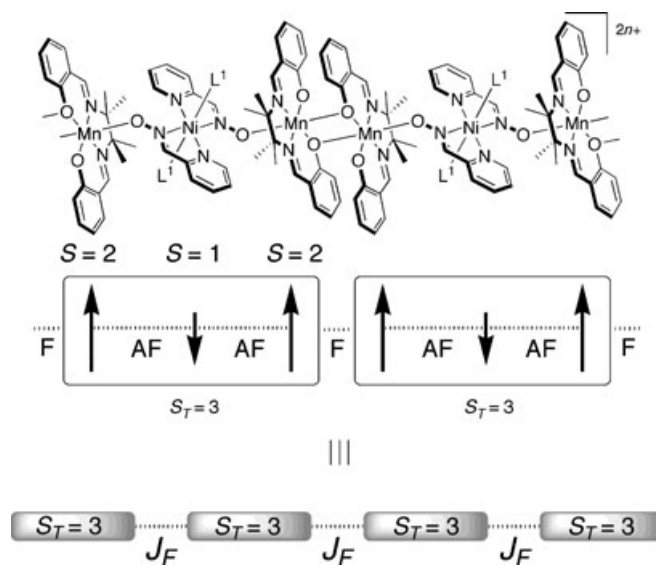
$$\tau(T) = \tau_0 \exp\left(\frac{\Delta_{\text{eff}}}{k_B T}\right) \quad (1)$$

Recently, a few 1D systems,<sup>[10–13]</sup> so-called single-chain magnets (SCMs),<sup>[11a]</sup> have also been reported, which exhibit a slow relaxation of the magnetization like SMMs. This behavior has been described in the framework of Glauber dynamics, developed in the 1960s for chains of ferromagnetically coupled Ising spins. According to this theoretical work, the relaxation time of the magnetization can be described [Eq. (2)]<sup>[14]</sup>, as  $\dot{H} = -2J_F S_T^2 \sum_i \sigma_i \sigma_{(i+1)}$ , where  $\tau_i$  is a pre-exponential factor introduced phenomenologically by Glauber to describe the individual reversal dynamics of Ising spins ( $S_T$ ) composing the chain,  $J_F$  is the ferromagnetic interaction between  $S_T$  spins along the chain, and  $\sigma = +1$  or  $-1$ .

$$\tau(T) = \tau_i(T) \exp\left(\frac{8J_F S_T^2}{k_B T}\right) \quad (2)$$

Recently, SCM behavior was reported for different type of chains (homo- or heterospin systems in ferro- or ferromagnetic arrangements),<sup>[10–13]</sup> and the Glauber theory has been treated as a rough approach to describe their magnetic behavior.<sup>[10,11a,13]</sup> Although a unified theoretical approach has not yet been developed for understanding the SCM behavior of all these materials, the series of 1D materials  $[\text{Mn}_2(\text{saltmen})_2\text{Ni}(\text{pao})_2(\text{L}^1)_2](\text{A})_2$  (saltmen<sup>2-</sup> = *N,N'*-(1,1,2,2-tetramethylethylene) bis(salicylideneimine)); pao<sup>-</sup> = pyridine-2-aldoximate;  $\text{L}^1$  = pyridine, 4-picoline, 4-*tert*-butylpyri-

dine, *N*-methylimidazole;  $\text{A} = \text{ClO}_4^-$ ,  $\text{BF}_4^-$ ,  $\text{PF}_6^-$ ,  $\text{ReO}_4^-$ ) offered us the opportunity to generalize Glauber’s approach in the case of a finite anisotropy  $D$ .<sup>[11b,c]</sup> Indeed, these compounds proved to be the prototypical SCM example of a chain with ferromagnetically coupled spins and finite anisotropy. Detailed experimental analyses of their magnetic behavior allowed us to estimate that the repeating spin units constituting the chains have an  $S_T = 3$  spin ground state, a large uniaxial anisotropy  $D/k_B \approx -2.5$  K, and are ferromagnetically coupled along the chain ( $J_F/k_B \approx +0.7$  K) (Scheme 1).<sup>[11a,b]</sup> Generalizing Glauber’s theory, we expressed the



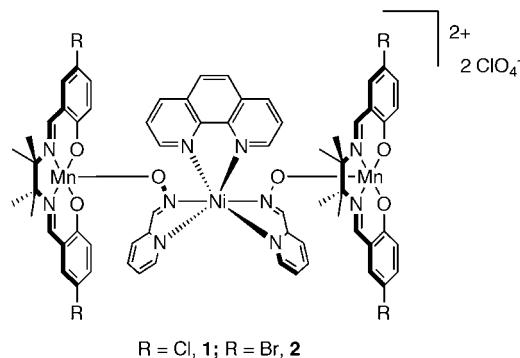
Scheme 1.

thermal variation of the relaxation time  $\tau(T)$  as a function of the characteristics of the repeating unit [Eq. (3)]<sup>[11b,c]</sup>, where  $\tau_0$  is a pre-exponential factor characteristic of the repeating unit.

$$\tau(T) = \tau_0 \exp\left[\frac{(8J_F + |D|)S_T^2}{k_B T}\right] \quad (3)$$

Therefore, the energy gap  $\Delta$  is no longer  $|D|S_T^2$  [or  $|D|(S_T^2 - 1/4)$ ] observed for an SMM, or  $8J_F S_T^2$  for an SCM with ferromagnetically coupled Ising spins, but  $(8J_F + |D|)S_T^2$  for the case of a SCM with ferromagnetically coupled anisotropic spins. In these compounds, the effective energy gap has been measured as  $\Delta_{\text{eff}}/k_B \approx 70$  K, which compares with a theoretical estimate of 73 K from  $(8J_F + |D|)S_T^2$ . Based on this work, we can imagine a case in which the repeating units of the previous chain are independently separated as  $J_F \approx 0$ . This would allow us 1) to probe directly their intrinsic magnetic characteristics ( $S_T$  and  $D$ ), and 2) to confirm the results reported for the SCM materials. Moreover, if the magnetic characteristics of these compounds are preserved when isolated, they should exhibit SMM behavior with an energy gap of  $\Delta_{\text{eff}}/k_B = |D|S_T^2 \approx 22$  K.

To probe these ideas, we synthesized two new Mn<sup>III</sup>-Ni<sup>II</sup>-Mn<sup>III</sup> trinuclear compounds: [Mn<sub>2</sub>(5-Rsaltmen)<sub>2</sub>Ni(pao)<sub>2</sub>(phen)](ClO<sub>4</sub>)<sub>2</sub> (R = Cl, **1**; Br, **2**). Here we describe the synthesis, crystal structures, and detailed magnetic properties of these compounds having a core in every respect similar to the repeat unit of the SCM materials introduced above.



## Results and Discussion

**Starting materials and synthesis of the trinuclear compounds:** In solution Mn<sup>III</sup> salen-type Schiff base complexes are present as an equilibrium mixture (Scheme 2) of a monomeric form [Mn(SB)(S)<sub>2</sub>]<sup>+</sup> and an out-of-plane dimeric form [Mn<sub>2</sub>(SB)<sub>2</sub>(S)<sub>2</sub>]<sup>2+</sup> (SB: salen-type Schiff base ligand, S: unidentate solvent ligand).<sup>[15]</sup> In the Mn/saltmen series, the dimeric species have in many cases been found in the solid state, although their geometry depends dramatically on packing and ligand-field donation of unidentate ligands (i.e., solvent molecules S or counter anions).<sup>[15]</sup> Therefore, it was not surprising to find that the freshly synthesized Mn/5-

Rsaltmen<sup>2-</sup> (R = Cl and Br) precursors adopt an out-of-plane dimeric geometry, [Mn<sub>2</sub>(5-Rsaltmen)<sub>2</sub>(H<sub>2</sub>O)<sub>2</sub>](ClO<sub>4</sub>)<sub>2</sub>, in the solid state, as shown in Figure 1a for R = Br. Nevertheless, the monomeric form [Mn(5-Rsaltmen)(MeOH)<sub>2</sub>]-

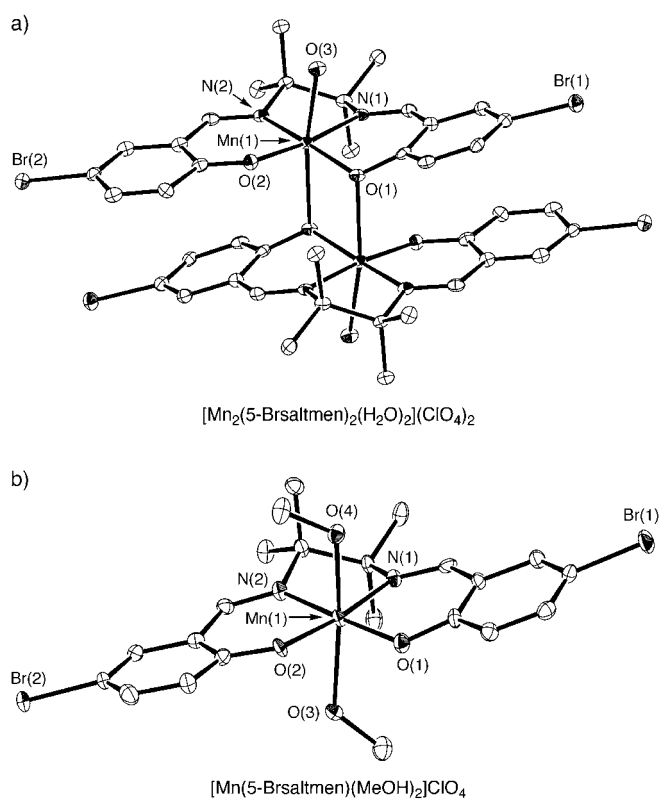
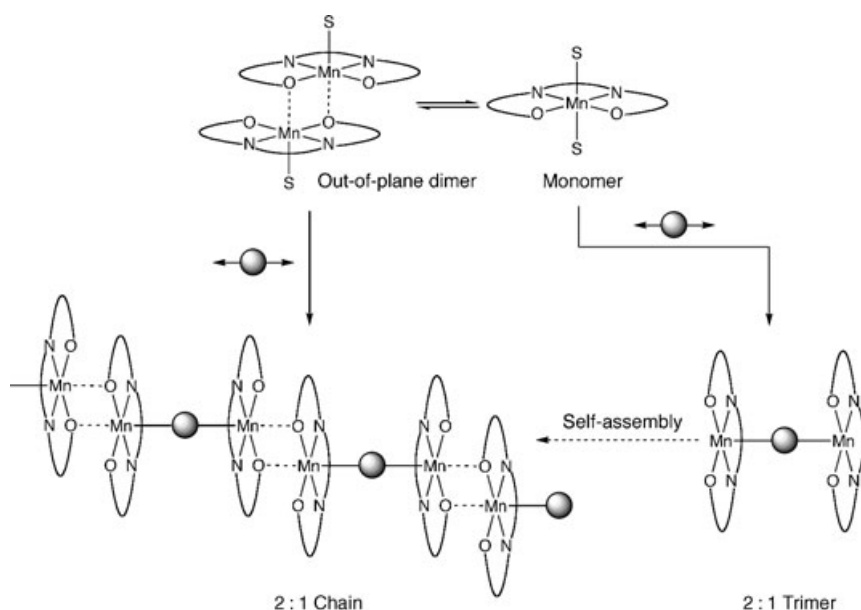


Figure 1. Structures of out-of-plane dimer (a) and monomer (b) for the Mn<sup>III</sup>(5-Brsaltmen) complex (50% probability thermal ellipsoids). Hydrogen atoms are omitted for clarity.

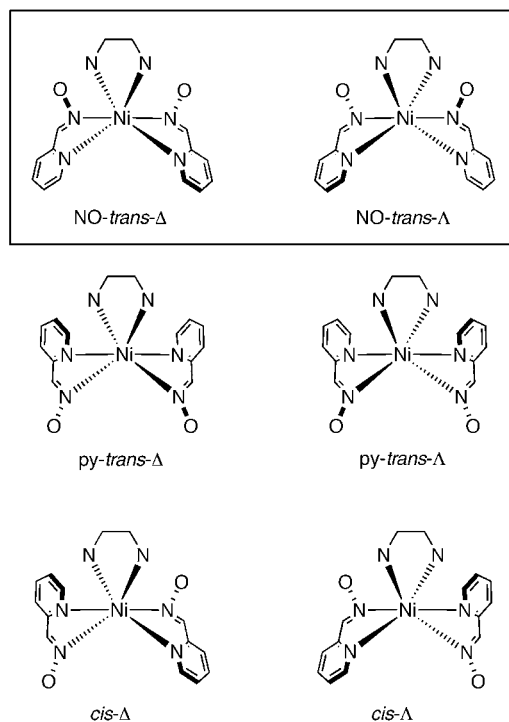


Scheme 2.

ClO<sub>4</sub> can be also isolated by recrystallizing the dimeric species from MeOH/water (Figure 1b for R = Br). Although both dimer and monomer could thus be involved in assembly reactions with a coordination donor, the present work is devoted to the assembly reaction of the out-of-plane dinuclear complexes [Mn<sub>2</sub>(5-Rsaltmen)<sub>2</sub>(H<sub>2</sub>O)<sub>2</sub>](ClO<sub>4</sub>)<sub>2</sub> (R = Cl, Br) with Ni<sup>II</sup> precursors (vide infra).

Ni<sup>II</sup> pyridine-2-aldoximate (pao<sup>-</sup>) complexes [Ni<sup>II</sup>(pao)<sub>2</sub>(bpy)] and [Ni<sup>II</sup>(pao)<sub>2</sub>(phen)] (bpy = 2,2'-bipyridine, phen = 1,10-phenanthroline),<sup>[16]</sup> were chosen as the coordination donor and used for the first time in assembly reactions.

These Ni complexes have six conformational isomers, namely, *NO-trans*-( $\Delta,\Delta$ ), *py-trans*-( $\Delta,\Delta$ ), and *cis*-( $\Delta,\Delta$ ), in which *trans* and *cis* are defined by the arrangement of the two  $\text{pao}^-$  ligands around the  $\text{Ni}^{\text{II}}$  ion (Scheme 3). Although these Ni complexes should be able to explore the different conformations in solution, both  $\text{Ni}^{\text{II}}$  precursors have always been isolated as a racemic mixture of the *NO-trans* conformations in the crystal.<sup>[16]</sup> The racemic mixture was employed in the following assembly reactions.



Scheme 3.

The assembly reactions of  $[\text{Mn}_2(5\text{-Rsaltmen})_2(\text{H}_2\text{O})_2](\text{ClO}_4)_2$  ( $\text{R}=\text{Cl}, \text{Br}$ ) with  $[\text{Ni}(\text{pao})_2(\text{L}^2)]$  ( $\text{L}^2=2,2'\text{-bpy}, 1,10\text{-phen}$ ) in a molar ratio of 1:2 were carried out in  $\text{MeOH}/\text{H}_2\text{O}$ .  $[\text{Ni}^{\text{II}}(\text{pao})_2(\text{bpy})]$  leads under most reaction conditions to a mixture of products. By using  $[\text{Mn}_2(5\text{-Brsaltmen})_2(\text{H}_2\text{O})_2](\text{ClO}_4)_2$  in the reaction, the 2:1 chain form, analogous to the  $[\text{Mn}_2(\text{saltmen})_2\text{Ni}(\text{pao})_2(\text{L}^1)_2](\text{A})_2$  series,<sup>[11a,b]</sup> was finally isolated.<sup>[17]</sup> A similar reaction with  $[\text{Mn}_2(5\text{-Clsaltmen})_2(\text{H}_2\text{O})_2](\text{ClO}_4)_2$  led to two cases of production of a mixture of 2:1 chain and 2:1 trimer species and production of 2:1 chain. The former was found when the reaction was carried out in  $\text{MeOH}/\text{H}_2\text{O}$ , in which the mixture ratio was strongly influenced by the reaction procedure, while the latter was found when it was carried out in  $\text{MeOH}/\text{EtOH}$ .<sup>[17]</sup>

When  $[\text{Ni}^{\text{II}}(\text{pao})_2(\text{phen})]$  was employed, trinuclear complexes  $[\text{Mn}_2(5\text{-Rsaltmen})_2\text{Ni}(\text{pao})_2(\text{phen})](\text{ClO}_4)_2 \cdot n\text{-solvent}$  ( $\text{R}=\text{Cl}, \mathbf{1}$ ;  $\text{Br}, \mathbf{2}$ ) are systematically and reproducibly obtained as brown needlelike microcrystalline materials in high yield. Single crystals for X-ray crystallography and magnetic measurements were obtained by slow diffusion in

$\text{MeOH}/\text{H}_2\text{O}$  (see Experimental Section). These synthetic results illustrate how the type of ligand (5-Rsaltmen or *bpy*/*phen*) influences the final architecture in these systems, for example, ligand field at the metal center, ligand–metal interaction, and packing effects.

**Structural description:** Compounds **1** and **2** were structurally characterized by single-crystal X-ray analysis. The two compounds are isostructural, having a similar unit cell and the same space group of  $P2_1/c$  (no. 14). ORTEP plots of the cations of **1** and **2** are depicted in Figure 2. Selected bond lengths and angles are summarized in Table 1. In the asymmetric cationic trinuclear unit, two  $[\text{Mn}^{\text{III}}(5\text{-Rsaltmen})]^+$  groups ( $\text{R}=\text{Cl}, \text{Br}$ ) and an  $\text{Ni}^{\text{II}}(\text{pao})_2(\text{phen})$  unit are linked through oximate bridges of the  $\text{Ni}^{\text{II}}$  moiety to form a  $[\text{Mn}^{\text{III}}\text{-ON-Ni}^{\text{II}}\text{-ON-Mn}^{\text{III}}]$  linear motif.

The  $\text{Ni}^{\text{II}}$  ion has a distorted octahedral coordination sphere with two bidentate  $\text{pao}^-$  and one *phen* molecule. Therefore the Ni moiety exhibits two chiral conformations  $\Delta$  and  $\Lambda$  in which the  $\text{pao}^-$  ligands are arranged in a *cis* mode with a *NO-trans* positions (see Scheme 3). The *NO-trans* forms of Ni precursor are thus preserved in the assembly process.<sup>[16]</sup> The oximate functions of the  $\text{Ni}(\text{pao})_2(\text{phen})$  moiety are coordinated to the  $\text{Mn}^{\text{III}}$  ion of  $[\text{Mn}(5\text{-Rsaltmen})]^+$  groups at their apical position with bond lengths and angles of  $\text{Mn}(1)\text{-O}(3)$  2.063(3), 2.065(4) Å;  $\text{Mn}(2)\text{-O}(4)$  2.062(3), 2.059(4) Å;  $\text{Mn}(1)\text{-O}(3)\text{-N}(3)$  136.2(2), 136.7(4)°; and  $\text{Mn}(2)\text{-O}(4)\text{-N}(5)$  136.3(2), 135.6(4)°, respectively, for **1** and **2**. Slightly smaller Mn–O–N bending angles (131.8–134.9°) and longer apical Mn– $\text{O}_{\text{oximate}}$  bond lengths (2.100–2.122 Å) were found in the family of  $[\text{Mn}_2(\text{saltmen})_2\text{Ni}(\text{pao})_2(\text{L}^1)_2](\text{A})_2$  compounds.<sup>[11a,b]</sup> Whereas the coordination sphere of the Mn sites in these 1D compounds is clearly octahedral with a Jahn–Teller distortion, the Mn ions in the present trinuclear compounds assume a square-pyramidal geometry. The vacant apical position of the usual octahedral  $\text{Mn}^{\text{III}}$  geometry is however weakly in contact with the 5-R ( $\text{R}=\text{Cl}, \text{Br}$ ) group of neighboring trimeric units ( $\text{Mn}(1)\cdots\text{Cl}(4)^*$  3.492(1),  $\text{Mn}(2)\cdots\text{Cl}(2)^{**}$  3.347(1) Å for **1**, and  $\text{Mn}(1)\cdots\text{Br}(4)^*$  3.561(1) and  $\text{Mn}(2)\cdots\text{Br}(2)^{**}$  3.418(1) Å for **2**, with the following symmetry operation: \*  $1+x, 1/2-y, 1/2+z$ ; \*\*  $-1+x, 1/2-y, -1/2+z$ ). The Mn $\cdots$ Cl distances are slightly shorter than the Mn $\cdots$ Br distances, in agreement with the higher electronegativity of Cl. The equatorial Mn–X bond lengths ( $\text{X}=\text{N}$  or  $\text{O}$  of the 5-Rsaltmen<sup>2-</sup> ligand) are in the range of 1.859(5)–1.990(6) Å, significantly shorter than the apical Mn– $\text{O}_{\text{oximate}}$  bond, as expected for a Jahn–Teller distortion.

The packing arrangement of the trinuclear units in **1** is shown in Figure 3 (the same view can be obtained for isostructural **2**). The Mn–Ni–Mn axes of the trinuclear units are located in the *ac* plane with a  $\cdots\Delta,\Delta,\Delta,\Delta\cdots$  alternating arrangement of the Ni moieties along the *c* axis, and  $\cdots\Delta,\Delta,\Delta,\Delta\cdots$  or  $\cdots\Lambda,\Lambda,\Lambda,\Lambda\cdots$  arrangements along the *a* axis. The shortest intermolecular metal–metal distance is 7.54 Å for **1** and 7.59 Å for **2** [ $\text{Mn}(1)\cdots\text{Mn}(2)$ ], found between molecules along the *a* axis (metal–metal distances between mol-

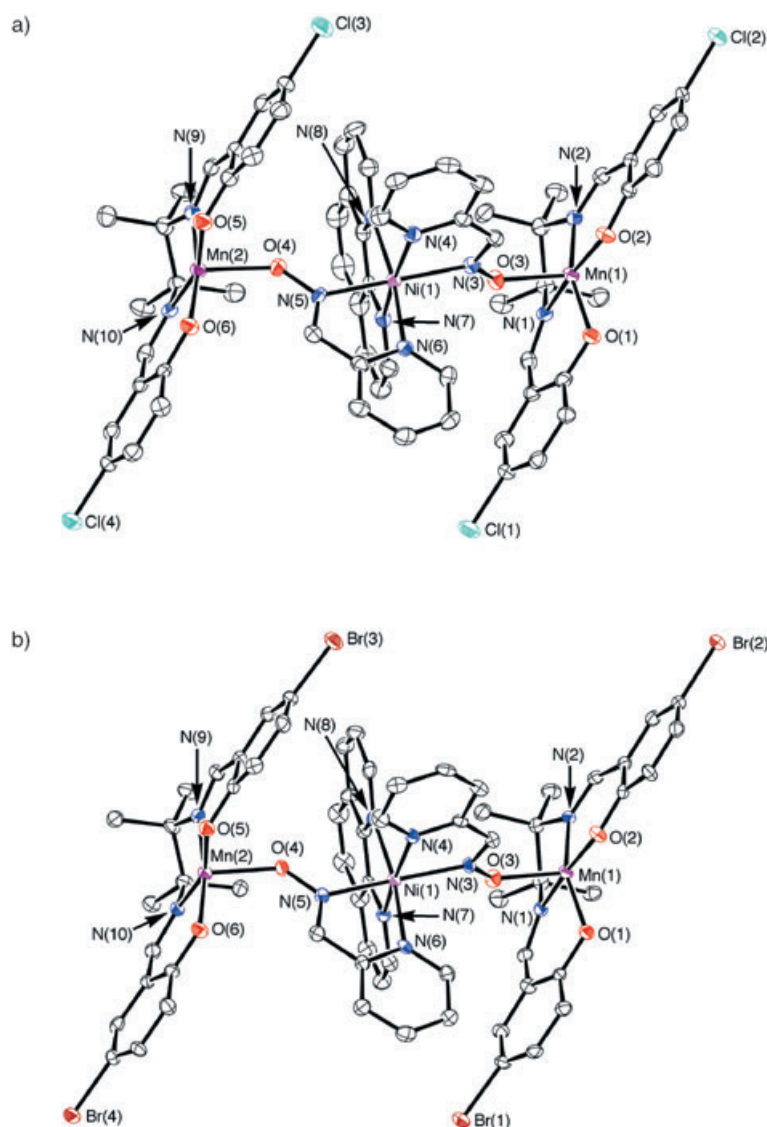


Figure 2. Structure of trinuclear Mn-Ni-Mn cations in a) **1** and b) **2** with the atomic numbering scheme for selected atoms (50% probability thermal ellipsoids). Hydrogen atoms are omitted for clarity.

ecules along the *c* axis range from 10.34 to 10.45 Å for **1**, and from 10.39 to 10.51 Å for **2**; and those in the *a*+*c* direction are 8.95 Å for **1** and 9.34 Å for **2**. Close contacts of the Mn ions with the 5-R atoms (R=Cl for **1** and Br for **2**) of neighboring molecules (dashed lines in Figure 3) form a quasi-1D chain. Furthermore,  $\pi$ - $\pi$  stacking of the phenyl rings of the 5-Rsaltmen<sup>2-</sup> ligand between neighboring molecules (C...C 3.27–3.54 Å for **1** and 3.26–3.63 Å for **2**) forms a two-dimensional array of trinuclear units.

**Magnetic properties:** The dc magnetic susceptibility was measured on a polycrystalline sample of **1** and **2** in the temperature range of 1.8–300 K at an applied field of 1 kOe. The magnetic properties of the two isostructural compounds are, as expected, almost identical and hence only the data of **1** are shown (see Supporting Information for **2**). Above 120 K, the susceptibility obeys the Curie–Weiss law with  $C=$

6.5 and 6.6 cm<sup>3</sup>K mol<sup>-1</sup> and  $\theta=-41$  and  $-42.4$  K for **1** and **2**, respectively. The Curie constants are in reasonable agreement with the value expected for a magnetically diluted spin system consisting of two  $S=2$  Mn<sup>III</sup> ions and one  $S=1$  Ni<sup>II</sup> ion. Moreover, the negative Weiss constant indicates the presence of dominant antiferromagnetic exchange interaction between spin carriers. As observed for the [Mn<sub>2</sub>(saltmen)<sub>2</sub>Ni(pao)<sub>2</sub>(L<sup>1</sup>)<sub>2</sub>](A)<sub>2</sub> series ( $\theta \approx -25$  to  $-35$  K), the Weiss constant principally reflects magnetic interactions between Mn<sup>III</sup> and Ni<sup>II</sup> through the oximato bridge.<sup>[11b]</sup> As shown in Figures 4 and S1 (Supporting Information),  $\chi T$  gradually decreases from 300 K (5.83 and 5.69 cm<sup>3</sup>K mol<sup>-1</sup> for **1** and **2**, respectively) to a minimum at about 72 K (4.83 and 4.68 cm<sup>3</sup>K mol<sup>-1</sup> for **1** and **2**). Below 72 K,  $\chi T$  first increases to reach a maximum at 22 K (5.18 and 4.98 cm<sup>3</sup>K mol<sup>-1</sup> for **1** and **2**) before its final decrease down to 1.17 and 1.27 cm<sup>3</sup>K mol<sup>-1</sup> at 1.82 K for **1** and **2**, respectively. Based on the structural description of **1** and **2** and the trinuclear nature of the compound, an Mn<sup>III</sup>-Ni<sup>II</sup>-Mn<sup>III</sup> model ( $S_{\text{Mn}}=2$ ,  $S_{\text{Ni}}=1$ ) was used to fit the magnetic data.<sup>[11a]</sup> A Heisenberg Hamiltonian was used to derive the susceptibility [Eq. (4)], where  $J$

is the exchange interaction between Mn<sup>III</sup> and Ni<sup>II</sup> ions through the –ON– bridge,  $S_{\text{T}}$  the total spin operator of the trimer ( $S_{\text{T}}=S_{\text{Mn1}}+S_{\text{Ni}}+S_{\text{Mn2}}$ ), and  $S_{\text{Tz}}$  is the projection of  $S_{\text{T}}$  along the magnetic field  $H_z$  applied in the *z* direction.

$$\hat{H} = -2J\{\hat{S}_{\text{Mn1}} \cdot \hat{S}_{\text{Ni}} + \hat{S}_{\text{Ni}} \cdot \hat{S}_{\text{Mn2}}\} + g\mu_{\text{B}}S_{\text{Tz}}H_z \quad (4)$$

Fitting of the experimental data was only possible down to 45 K and led to a first estimation of  $J$  of around  $-22$  K for both compounds. Although this model was able to reproduce qualitatively the minimum of  $\chi T$ , this was not the case for its final decrease below 22 K (Figure 4, blue line). Antiferromagnetic interactions between trinuclear units (resulting from intermolecular  $\pi$ - $\pi$  stacking and Mn...X weak contacts that mainly produce a two-dimensional interacting network, as shown in Figure 3) and anisotropic effects (induced



Table 1. Bond lengths [Å] and angles [°] around metal ions for **1** and **2** with estimated standard deviations in parentheses.

Atom	<b>1</b>	<b>2</b>	Atom	<b>1</b>	<b>2</b>
Mn1–O1	1.877(3)	1.876(5)	Mn1–O2	1.872(2)	1.859(5)
Mn1–N1	1.983(3)	1.974(5)	Mn1–N2	1.985(3)	1.976(5)
Mn1–O3	2.063(3)	2.065(4)	Mn1...X4 <sup>[a]</sup>	3.492(1)	3.561(1)
Mn2–O5	1.882(3)	1.888(5)	Mn2–O6	1.891(3)	1.884(5)
Mn2–N9	1.985(3)	1.990(6)	Mn2–N10	1.987(3)	1.978(6)
Mn2–O4	2.062(3)	2.059(4)	Mn2...X2 <sup>[b]</sup>	3.347(1)	3.418(1)
Ni1–N3	2.059(3)	2.060(5)	Ni1–N4	2.069(3)	2.073(5)
Ni1–N5	2.054(3)	2.057(5)	Ni1–N6	2.082(3)	2.090(5)
Ni1–N7	2.057(3)	2.059(6)	Ni1–N8	2.085(3)	2.089(6)
Ni1–N3–O3	123.3(2)	124.0(4)	N4–Ni1–N3	79.0(1)	79.1(2)
N5–Ni1–N3	172.6(1)	172.4(2)	N6–Ni1–N3	97.3(1)	97.1(2)
N7–Ni1–N3	93.5(1)	93.4(2)	N8–Ni1–N3	89.8(1)	90.1(2)
N5–Ni1–N4	94.9(1)	95.0(2)	N6–Ni1–N4	91.4(1)	92.5(2)
N7–Ni1–N4	170.7(1)	170.2(2)	N8–Ni1–N4	94.0(1)	93.3(2)
Ni1–N5–O4	122.7(2)	122.9(4)	N6–Ni1–N5	78.6(1)	78.2(2)
N7–Ni1–N5	92.9(1)	93.0(2)	N8–Ni1–N5	94.8(1)	95.1(2)
N7–Ni1–N6	95.1(1)	94.7(2)	N8–Ni1–N6	171.8(1)	171.5(2)
N8–Ni1–N7	80.3(1)	80.3(2)	O3–Mn1–O1	92.4(1)	92.8(2)
O2–Mn1–O1	90.6(1)	91.2(2)	N1–Mn1–O1	92.0(1)	91.7(2)
N2–Mn1–O1	156.5(1)	155.7(2)	O3–Mn1–O2	103.2(1)	102.5(2)
N1–Mn1–O2	169.4(1)	170.2(2)	N2–Mn1–O2	92.3(1)	92.3(2)
Mn1–O3–N3	136.2(2)	136.7(4)	N1–Mn1–O3	87.0(1)	86.7(2)
N2–Mn1–O3	109.5(1)	109.9(2)	N2–Mn1–N1	81.3(1)	81.3(2)
Mn2–O4–N5	136.3(2)	135.6(4)	O5–Mn2–O4	91.1(1)	92.3(2)
O6–Mn2–O4	103.0(1)	102.0(2)	N9–Mn2–O4	87.9(1)	87.8(2)
N10–Mn2–O4	106.0(1)	107.0(2)	O6–Mn2–O5	92.1(1)	93.0(2)
N9–Mn2–O5	91.6(1)	91.1(2)	N10–Mn2–O5	160.8(1)	158.4(2)
N9–Mn2–O6	168.3(1)	169.2(2)	N10–Mn2–O6	92.4(1)	92.5(2)
N10–Mn2–N9	80.7(1)	80.1(2)			

[a] Symmetry operation:  $1+x, 1/2-y, 1/2+z$ . [b] Symmetry operation:  $-1+x, 1/2-y, -1/2+z$ .

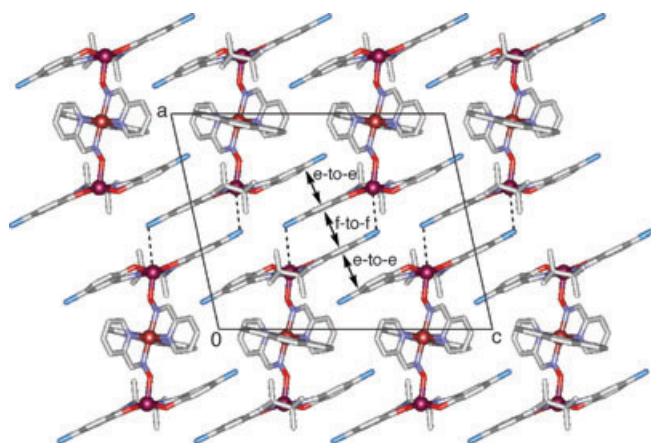


Figure 3. Packing diagram of **1** projected on the  $ac$  plane. The edge-to-edge (e-to-e) and face-to-face (f-to-f)  $\pi$ - $\pi$  stacking interactions are labeled. Dashed lines indicate Mn...Cl contacts.

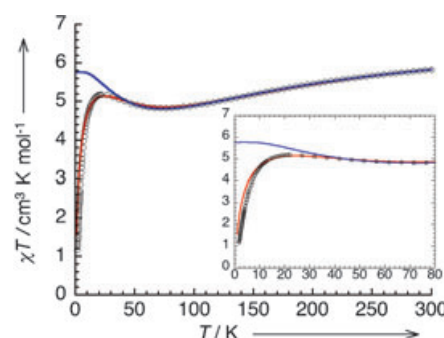


Figure 4. Temperature dependence of  $\chi T$  for **1** at 1 kOe. The solid blue and red lines are the fits for model with Heisenberg Mn-Ni-Mn trinuclear units and the same model taking into account interactions between these units in the mean-field approximation, respectively (see text). Inset: Enlarged view of the low-temperature region.

by the zero-field splitting, ZFS, of the metal ions) are probably responsible for the low-temperature magnetic behavior and hence should be taken into account. Therefore, as a first approach, intertrinuclear interactions were introduced in the previous model in the mean-field approximation [Eq. (5)]<sup>[18]</sup>, where  $z$  is the number of next-neighbour trinuclear units and  $J'$  is the average magnetic interaction between trinuclear compounds.

$$\chi = \frac{\chi_{\text{trinuclear}}}{1 - \frac{2zJ'}{Ng^2\mu_B} \chi_{\text{trinuclear}}} \quad (5)$$

As shown Figure 4 (red line), this model reproduces qualitatively well the magnetic data with  $J/k_B = -24.3(1)$  K,  $g = 2.00(2)$ , and  $zJ/k_B = -0.18(2)$  K for **1** (with  $J/k_B = -24.0(1)$  K,  $g = 1.97(2)$ , and  $zJ/k_B = -0.19(2)$  K for **2**). The obtained  $J$  values are in good agreement with those estimated for related materials. Indeed,  $J$  has been estimated to range between  $-21$  and  $-26$  K in the family of SCMs  $[\text{Mn}_2(\text{saltmen})_2\text{Ni}(\text{pao})_2(\text{L}^1)_2](\text{A})_2$ <sup>[11a,b]</sup> and in a series of Ni-Mn-Mn-Ni tetranuclear complexes  $[\text{Mn}(5\text{-R-saltmen})\text{Ni}(\text{pao})(\text{bpy})_2](\text{ClO}_4)_4$  ( $\text{R} = \text{H}, \text{Cl}, \text{Br}, \text{MeO}$ ).<sup>[19]</sup> The antiferromagnetic interaction  $J$  between  $\text{Mn}^{\text{III}}$  and  $\text{Ni}^{\text{II}}$  ions via  $-\text{ON}-$  bridges leads to an  $S_T = 3$  ground state for both trinuclear compounds. As seen in Figure 4 below 10 K, antiferromagnetic interactions between trimers evaluated around  $-0.2$  K are not able to completely reproduce the experimental data, that is, the anisotropy may be relevant to improving the model. Instead of making a heavy numerical procedure to model the susceptibility including  $J$ ,  $g$ ,  $zJ$ , and  $D$ , a detailed analysis of the dependence on magnetization field was made to determine these two last parameters.

The field dependence of the magnetization was measured up to 70 kOe and down to 1.82 K (Figure 5 for **1** and Figure S2 for **2** (Supporting Information)) without observation of hysteresis. At this lowest temperature and before a quasilinear regime of the magnetization above 40 kOe, a step in the field dependence appears at 9.986 and 9.380 kOe, respectively, for **1** and **2** (values obtained from  $dM/dH$  versus  $H$

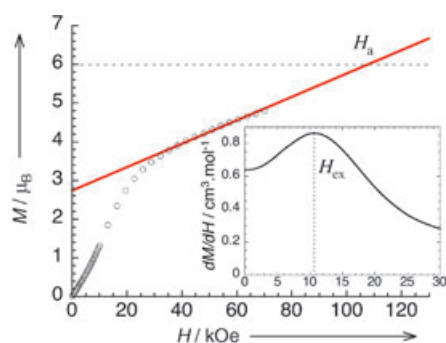


Figure 5. Field dependence of the magnetization for **1** at 1.82 K. The dashed line represents the expected saturation of the magnetization at  $M_{\text{sat}} = gS_T$ , where  $g$  is the Landé factor deduced from the  $\chi T$  fitting (Table 2). The solid red line is a linear fit of the high-field magnetization, and its intersection with  $M_{\text{sat}}$  corresponds to  $H_a$ . Inset: Numerical derivative of  $M$  relative to  $H$  as a function of  $H$ .

plots, inset to Figure 5 and Figure S2 in the Supporting Information). By attributing this field  $H_{\text{ex}}$  to a field induced parallel alignment of antiferromagnetic coupled  $S_T = 3$  trinuclear units,<sup>[20]</sup>  $zJ'$  can be estimated at  $-0.22(2)$  and  $-0.21(2)$  K for **1** and **2**, respectively.<sup>[21,22]</sup> These values are in excellent agreement with those deduced from the mean-field approach (vide supra) used to fit the temperature dependence of the susceptibility. Moreover, these intertrinuclear interactions would eventually lead to long-range antiferromagnetic ordering at a critical temperature roughly estimated (from the mean-field approximation:  $T_N = 2zJS_T(S_T + 1)/3k_B$ ) as 1.76 and 1.66 K for **1** and **2** respectively. Therefore, at 1.82 K these compounds are probably not in their long-range antiferromagnetic ordered state but are nevertheless strongly correlated. In this case, the short-range order allows us to estimate the intertrinuclear interactions. Above 40 kOe, the magnetization linearly increases with increasing applied field to reach 4.8 and 4.7  $\mu_B$  at 70 kOe for **1** and **2**, respectively. The fact that saturation is not observed up to 70 kOe highlights the strong anisotropy of the material. Considering that above 40 kOe only the hard direction of the anisotropy still resists the field alignment of the magnetization,<sup>[23]</sup>  $D$  can be estimated by extrapolating the linear behavior of the magnetization to its value at complete saturation  $M_{\text{sat}} = gS_T$ . The anisotropic fields were estimated to be  $H_a \approx 107$  kOe for **1** and 109 kOe for **2**. These values yield an anisotropic parameter  $D$  for the trinuclear unit close to  $-2.40(5)$  K in both cases.<sup>[24]</sup> To confirm this result,  $D$  was also obtained from the analysis of the reduced magnetization plot  $M$  versus  $H/T$  by taking into account that only the ground state  $S_T = 3$  is populated in the experimental temperature range of 1.8–4.5 K and between 40 and 70 kOe<sup>[20]</sup> (Figure 6 for **1** and Figure S3 in the Supporting Information for **2**). Without ZFS contribution, the various isofield magnetization curves should be superimposed and  $M$  would saturate at  $M_{\text{sat}}$ . The nonsuperimposition of these plots clearly indicates the presence of ZFS. As seen in Figure 6, their numerical simulations yielded  $D/k_B = -2.30(5)$  and  $-2.31(5)$  K for **1** and **2**, respectively. These

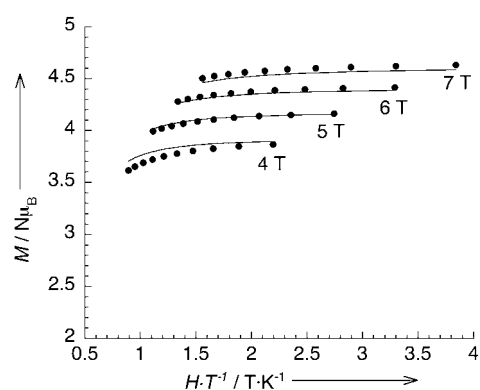


Figure 6. Plot of  $M$  versus  $H/T$  for **1** in the temperature range below 4.5 K. The solid lines are simulated curves (see text).

values are in very good agreement with those estimated from  $H_a$  and also very close to those reported for  $[\text{Mn}_2(\text{saltmen})_2\text{Ni}(\text{pao})_2(\text{py})_2](\text{ClO}_4)_2$  ( $D/k_B = -2.5$  K).<sup>[11c]</sup> The detailed analysis of the dc magnetic measurements has clearly established the magnetic characteristics of these trinuclear  $S_T = 3$  anisotropic compounds ( $J$ ,  $g$ , and  $D$ ) and also the magnetic interaction between them ( $zJ$ ). All these parameters are summarized in Table 2.

Table 2. Magnetic characteristics of the trinuclear complexes **1** and **2**.

	<b>1</b>	<b>2</b>
$J/k_B$ [K]	$-24.3(1)$	$-24.0(1)$
$g$	$2.00(2)$	$1.97(2)$
$D/k_B$ [K] <sup>[a]</sup>	$-2.4(5)$	$-2.4(5)$
$D/k_B$ [K] <sup>[b]</sup>	$-2.30(5)$	$-2.31(5)$
$zJ/k_B$ [K] <sup>[c]</sup>	$-0.18(2)$	$-0.19(2)$
$zJ/k_B$ [K] <sup>[a]</sup>	$-0.22(2)$	$-0.21(2)$
$\Delta/k_B$ [K] <sup>[d]</sup>	$21.1(1)$	$21.2(1)$
$\tau_0$ [s] <sup>[e]</sup>	$1.2(1) \times 10^{-7}$	$1.5(1) \times 10^{-7}$
$\Delta_{\text{eff}}/k_B$ [K] <sup>[e]</sup>	$18.3(1)$	$18.2(1)$

[a] From analysis of  $M$  versus  $H$  curves. [b] From plots of reduced magnetization. [c] From analysis of the temperature dependence of the magnetic susceptibilities. [d] Calculated from the average value of the  $D$  parameters reported in this table. [e] Deduced from analysis of the ac susceptibility (see Figure 8).

As observed for single-molecule magnets, the presence of a uniaxial anisotropy  $D$  creates an energy barrier  $\Delta/k_B = |D| S_T^2$  between the two  $m_s = \pm 3$  levels. From the magnetic characteristics of **1** and **2** deduced from the dc measurements,  $\Delta/k_B$  can be estimated to be around 21 K (Table 2), and therefore SMM behavior should be observed. To probe this possibility, the ac magnetic susceptibility was measured in these two compounds. The measurements were performed on polycrystalline samples of **1** and **2** in the temperature range of 1.8–5 K at zero dc field and with an 3 Oe ac field. In-phase ( $\chi'$ ) and out-of-phase ( $\chi''$ ) components of the ac susceptibility are shown in Figure 7 for **1** and in Figure S4 in the Supporting Information for **2**. As expected for an SMM, both  $\chi'$  and  $\chi''$  components are strongly dependent on fre-

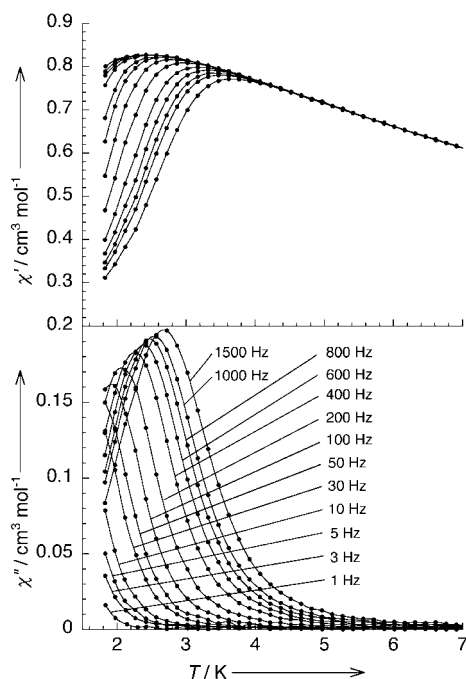


Figure 7. Temperature and frequency dependence of the real ( $\chi'$ ) and imaginary ( $\chi''$ ) parts of the ac susceptibility for **1**. The solid lines are guides for eye.

quency  $\nu$ , and a single relaxation mode of the magnetization is observed.

Experimentally, the temperature dependence of the relaxation time  $\tau$  can be obtained at a given frequency, from the temperature of the maximum in the  $\chi''$  versus  $T$  plot, also called the blocking temperature  $T_B$  ( $\tau(T_B) = 1/2\pi\nu$ ). Therefore, plots of  $\tau$  versus  $1/T$  can be deduced for **1** and **2** (Figure 8). Between 3 and 1.8 K, the relaxation time follows an Arrhenius behavior with effective activation energies  $\Delta_{\text{eff}}/k_B$  of 18.3(1) and 18.2(1) K and pre-exponential factors  $\tau_0$  of  $1.2(1) \times 10^{-7}$  and  $1.5(1) \times 10^{-7}$  s for **1** and **2**, respectively. The  $\Delta_{\text{eff}}/k_B$  values are slightly lower than that of  $\Delta/k_B = 21$  K

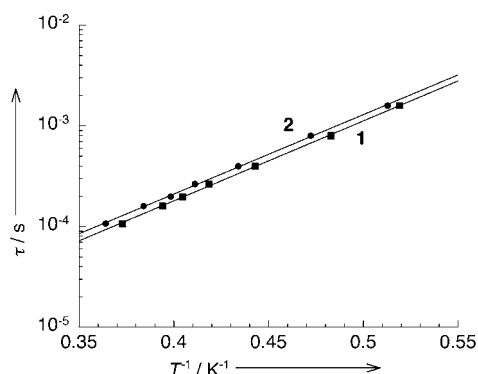


Figure 8. Semilog plot of relaxation time  $\tau$  vs  $1/T$  for **1** and **2**. The solid line represents the least-squares linear fit of the experimental data with the Arrhenius law (see text). The best-fit parameters are listed in Table 2.

calculated from the ZFS parameters and the spin ground state of these compounds (Table 2). This was already noted in other SMM systems<sup>[4a]</sup> and has been attributed to quantum tunneling of the magnetization, which allows the magnetization to find an alternative route of relaxation. Therefore, this effect reduced the thermal energy barrier found experimentally at low temperatures.

## Conclusion

Two  $\text{Mn}^{\text{III}}\text{-Ni}^{\text{II}}\text{-Mn}^{\text{III}}$  linear trinuclear compounds **1** and **2** have been synthesized, structurally characterized, and magnetically investigated. These complexes have the same  $[\text{Mn-ON-Ni-NO-Mn}]$  core as the repeating unit of the 1D chain compounds  $[\text{Mn}_2(\text{saltmen})_2\text{Ni}(\text{pao})_2(\text{L}')_2](\text{A})_2$ . For these 1D materials, the slow relaxation of the magnetization (i.e., SCM behavior) was first described on the basis of Glauber's theory<sup>[14]</sup> for chains of ferromagnetically coupled Ising spins.<sup>[11a]</sup> Since the repeating unit has experimentally a finite anisotropy  $D$ , the theory was extended to chains of ferromagnetically coupled anisotropic spins with a generalized description that explained well the experimentally observed relaxation of magnetization.<sup>[11b,c]</sup> Therefore, the magnetic characteristics of this repeating unit (i.e., spin ground state and anisotropy) play a crucial role in obtaining and understanding SCM behavior. In the present work, these characteristics were directly obtained by investigating a discrete unit of **1** and **2** having effectively an  $S_T = 3$  ground state with a large uniaxial anisotropy around  $-2.4$  K. These results thus confirm the corresponding parameters obtained indirectly for the repeat unit of the SCM materials and verify the validity of the hypothesis made to describe the SCM behavior. Moreover, as we expected, ac magnetic measurements established that **1** and **2** display single-molecule magnet behavior due to their  $S_T = 3$  ground state and uniaxial anisotropy. Despite the fact that such SMM behavior is relatively rare and has so far been seen only in a few heterometallic systems,<sup>[9]</sup> a more interesting point is the perspective opened by this study; it suggests that SCMs can be designed by connecting ferromagnetic SMMs into 1D chains. Doubtless this strategy will be explored in the near future and may lead to new SCMs with high blocking temperatures.

## Experimental Section

**General procedures and materials:** All chemicals and solvents used in the syntheses were of reagent grade. The ligand  $\text{H}_2\text{5-Rsaltmen}$  ( $\text{R} = \text{Cl}, \text{Br}$ ) was synthesized by reaction of 5-bromo- or 5-chlorosalicylaldehyde with 1,1,2,2-tetramethylethylenediamine in methanol/water.  $[\text{Ni}(\text{pao})_2(\text{phen})] \cdot n$  solvent ( $\text{pao}^- = \text{pyridine-2-aldoximate}$ ,  $\text{phen} = 1,10\text{-phenanthroline}$ ) were also prepared according to literature methods.<sup>[16]</sup>

**$[\text{Mn}_2(\text{5-Rsaltmen})_2(\text{H}_2\text{O})_2](\text{ClO}_4)_2$  ( $\text{R} = \text{Cl}, \text{Br}$ ):**  $\text{Mn}(\text{O}_2\text{CCH}_3)_3 \cdot 2\text{H}_2\text{O}$  (1.34 g, 10 mmol) and then  $\text{NaClO}_4$  (624 mg, 5.1 mmol) were added to a boiling methanol solution (80 mL) containing 5 mmol of  $\text{H}_2\text{5-Rsaltmen}$  (3.38 g,  $\text{R} = \text{Br}$ ; 1.97 g,  $\text{R} = \text{Cl}$ ). The resulting solution was stirred at



about 50°C for 30 min, and then water (30 mL) was slowly added during heating. After filtration, the filtrate was allowed to stand at room temperature for one week to form block crystals of  $[\text{Mn}_2(5\text{-Rsaltmen})_2(\text{H}_2\text{O})_2](\text{ClO}_4)_2$  (31% for R=Cl, 72% for R=Br).  $[\text{Mn}_2(5\text{-Clsaltmen})_2(\text{H}_2\text{O})_2](\text{ClO}_4)_2 \cdot 2\text{H}_2\text{O}$ : elemental analysis (%) calcd for  $\text{C}_{40}\text{H}_{44}\text{N}_4\text{O}_{16}\text{Cl}_6\text{Mn}_2$ : C 41.44, H 3.83, N 4.83; found: C 41.27, H 3.89, N 4.79; IR (KBr):  $\tilde{\nu}=1605$  ( $\nu_{\text{C-N}}$ );  $\tilde{\nu}=1067, 1099, 1123, 1148$  ( $\nu_{\text{Cl-O}}$ )  $\text{cm}^{-1}$ ; magnetic measurements:  $J_{\text{intradimer}}/k_{\text{B}}=1.6$  K,  $D_{\text{Mn}}/k_{\text{B}}=-2.5$  K,  $zJ_{\text{interdimer}}/k_{\text{B}}=-0.30$  K, and  $g=2.05$  with  $H=g\mu_{\text{B}}H(S_1+S_2)-2J_{\text{dimer}}S_1\cdot S_2+D_{\text{Mn}}[S_{1z}^2+S_{2z}^2]$  and Equation (5) applied to the case of a dimer.<sup>[18]</sup>  $[\text{Mn}_2(5\text{-Brsaltmen})_2(\text{H}_2\text{O})_2](\text{ClO}_4)_2$ : elemental analysis (%) calcd for  $\text{C}_{40}\text{H}_{44}\text{N}_4\text{O}_{14}\text{Br}_2\text{Cl}_2\text{Mn}_2$ : C 36.81, H 3.40, N 4.29; found: C 36.94, H 3.48, N 4.10; IR (KBr):  $\tilde{\nu}=1602$  ( $\nu_{\text{C-N}}$ ); 1069, 1108, 1146 ( $\nu_{\text{Cl-O}}$ )  $\text{cm}^{-1}$ ; magnetic measurements:  $J_{\text{intradimer}}/k_{\text{B}}=1.1$  K,  $D_{\text{Mn}}/k_{\text{B}}=-2.6$  K,  $zJ_{\text{interdimer}}/k_{\text{B}}=-0.24$  K, and  $g=1.95$  with  $H=g\mu_{\text{B}}H(S_1+S_2)-2J_{\text{dimer}}S_1\cdot S_2+D_{\text{Mn}}[S_{1z}^2+S_{2z}^2]$  and Equation (5) applied to the case of a dimer.<sup>[18]</sup>

**$[\text{Mn}(5\text{-Brsaltmen})(\text{MeOH})_2]\text{ClO}_4$** : Recrystallization of  $[\text{Mn}_2(5\text{-Brsaltmen})_2(\text{H}_2\text{O})_2](\text{ClO}_4)_2$  crystals from MeOH/H<sub>2</sub>O leads to the formation of  $[\text{Mn}(5\text{-Brsaltmen})(\text{MeOH})_2]\text{ClO}_4$ , which was confirmed by single-crystal X-ray crystallography (vide infra).

**$[\text{Mn}_2(5\text{-Clsaltmen})_2\text{Ni}(\text{pao})_2(\text{phen})](\text{ClO}_4)_2$  (1)**: A methanol solution (20 mL) of  $[\text{Ni}(\text{pao})_2(\text{phen})_2] \cdot 2\text{CHCl}_3 \cdot 1.5\text{H}_2\text{O}$  (182 mg, 0.25 mmol) was added to a methanol solution (20 mL) of  $[\text{Mn}_2(5\text{-Clsaltmen})_2(\text{H}_2\text{O})_2](\text{ClO}_4)_2 \cdot 2\text{H}_2\text{O}$  (141 mg, 0.12 mmol). After stirring for 1 min, water (10 mL) was added to the mixture, and the solution filtered. Pale brown microcrystals precipitated (146 mg, 71% based on Mn) overnight at room temperature while stirring. Single crystals of **1** were obtained by diffusion (Mn precursor in MeOH, Ni precursor in water). Elemental analysis (%) calcd for  $1 \cdot 4\text{H}_2\text{O}$ ,  $\text{C}_{64}\text{H}_{66}\text{N}_{10}\text{O}_{18}\text{Cl}_6\text{Mn}_2\text{Ni}$ : C 46.74, H 4.05, N 8.52; found: C 46.70, H 3.85, N 8.64; IR (Nujol):  $\tilde{\nu}=1600$  ( $\nu_{\text{C-N}}$ );  $\tilde{\nu}_{\text{Cl-O}}=1099$   $\text{cm}^{-1}$ .

**$[\text{Mn}_2(5\text{-Brsaltmen})_2\text{Ni}(\text{pao})_2(\text{phen})](\text{ClO}_4)_2$  (2)**: A methanol solution (20 mL) of  $[\text{Ni}(\text{pao})_2(\text{phen})_2] \cdot 2.5\text{CHCl}_3$  (195 mg, 0.25 mmol) was added to a methanol solution (20 mL) of  $[\text{Mn}_2(5\text{-Brsaltmen})_2(\text{H}_2\text{O})_2](\text{ClO}_4)_2$  (163 mg, 0.13 mmol). Water (10 mL) was added to the mixture, and the solution immediately filtered. The mixture was allowed to stand for several days at room temperature to form brown needle-type crystals (180 mg, 78% based on Mn). Single-crystals of **2** were obtained by diffusion (Mn precursor in MeOH/Ni precursor in water). Elemental analysis (%) calcd for  $2 \cdot 6\text{H}_2\text{O}$ ,  $\text{C}_{64}\text{H}_{70}\text{N}_{10}\text{O}_{20}\text{Br}_4\text{Cl}_6\text{Mn}_2\text{Ni}$ : C 41.36, H 3.80, N 7.54; found: C 41.24, H 3.72, N 7.63; IR (Nujol):  $\tilde{\nu}=1590$  ( $\nu_{\text{C-N}}$ );  $\tilde{\nu}_{\text{Cl-O}}=1097$   $\text{cm}^{-1}$ .

**Physical measurements**: Infrared spectra were measured on KBr disks or Nujol mulls with a Shimadzu FT-IR-8600 spectrophotometer. Magnetic susceptibilities were measured with a Quantum Design SQUID magnetometer MPMS-XL; dc measurements were collected from 1.8 to 300 K and from -70 kOe to 70 kOe; ac measurements were performed at various frequencies from 1 to 1488 Hz with an ac field amplitude of 3 Oe and no dc field applied. The general measurements were performed on finely ground polycrystalline samples. Experimental data were corrected for the sample holder and for the diamagnetic contribution calculated from Pascal constants.<sup>[25]</sup>

**Crystallography**: Single crystals of  $[\text{Mn}_2(5\text{-Brsaltmen})_2(\text{H}_2\text{O})_2](\text{ClO}_4)_2$ ,  $[\text{Mn}(5\text{-Brsaltmen})(\text{MeOH})_2]\text{ClO}_4$ , **1**, and **2** were prepared as described in the synthetic procedures. Single crystals were mounted on a glass rod. The crystal dimensions were  $0.2 \times 0.2 \times 0.8$  mm for  $[\text{Mn}_2(5\text{-Brsaltmen})_2(\text{H}_2\text{O})_2](\text{ClO}_4)_2$ ,  $0.1 \times 0.15 \times 0.2$  mm for  $[\text{Mn}(5\text{-Brsaltmen})(\text{MeOH})_2]\text{ClO}_4$ ,  $0.10 \times 0.02 \times 0.01$  mm for **1**, and  $0.20 \times 0.02 \times 0.02$  mm for **2**. The measurement temperature was  $93 \pm 1$  K for all compounds. Data were collected on a Rigaku CCD diffractometer (Saturn70) with graphite-monochromated  $\text{MoK}\alpha$  radiation ( $\lambda=0.71069$  Å). The structures were solved by direct methods (SIR97)<sup>[26]</sup> and expanded by Fourier techniques (DIRDIF99).<sup>[27]</sup> The non-hydrogen atoms were refined anisotropically, while hydrogen atoms were introduced as fixed contributors. Full-matrix least-squares refinements on  $F^2$  based on 5117 for  $[\text{Mn}_2(5\text{-Brsaltmen})_2(\text{H}_2\text{O})_2](\text{ClO}_4)_2$ , 4897 for  $[\text{Mn}(5\text{-Brsaltmen})(\text{MeOH})_2]\text{ClO}_4$ , 12576 for **1**, and 12577 observed reflections for **2** and 318, 345, 978, and 909 variable parameters, respectively, converged with unweighted and weighted agree-

ment factors of  $R1 = \sum ||F_o| - |F_c|| / \sum |F_o|$  ( $I > 2.00\sigma(I)$  and all data) and  $wR2 = [\sum w(F_o^2 - F_c^2)^2 / \sum w(F_o^2)^2]^{1/2}$  (all data). A Sheldrick weighting scheme was used. Neutral atom scattering factors were taken from Cromer and Waber.<sup>[28]</sup> Anomalous dispersion effects were included in  $F_{\text{calc}}$ ; the values  $\Delta f'$  and  $\Delta f''$  were those of Creagh and McAuley.<sup>[29]</sup> The values for the mass attenuation coefficients are those of Creagh and Hubbel.<sup>[30]</sup> All calculations were performed with the CrystalStructure crystallographic software package.<sup>[31]</sup>

**Crystal data for  $[\text{Mn}_2(5\text{-Brsaltmen})_2(\text{H}_2\text{O})_2](\text{ClO}_4)_2$** :  $\text{C}_{40}\text{H}_{44}\text{N}_4\text{O}_{14}\text{Cl}_2\text{Br}_4\text{Mn}_2$ ,  $M=1305.20$ , monoclinic  $P2_1/c$  (no. 14),  $a=7.349(4)$ ,  $b=15.684(9)$ ,  $c=19.415(12)$  Å,  $\beta=90.275(7)^\circ$ ,  $V=2237.8(23)$  Å<sup>3</sup>,  $Z=2$ ,  $\rho_{\text{calc}}=1.937$  g cm<sup>-3</sup>,  $F_{000}=1296.00$ ,  $2\theta_{\text{max}}=62.1^\circ$ . Final  $R1=0.041$  ( $I > 2.00\sigma(I)$ ),  $R1=0.056$  (all data),  $wR2=0.107$  (all data), GOF=1.014 for 318 parameters and a total of 20527 reflections, 6295 of which were unique ( $R_{\text{int}}=0.043$ ). The linear absorption coefficient  $\mu$  for  $\text{MoK}\alpha$  radiation was 43.38 cm<sup>-1</sup>. Application of an empirical absorption correction resulted in transmission factors ranging from 0.62 to 1.00. The data were corrected for Lorentzian and polarization effects. Max. positive and negative peaks in  $\Delta F$  map were  $\rho_{\text{max}}=1.18$  e Å<sup>-3</sup> and  $\rho_{\text{min}}=-0.96$  e Å<sup>-3</sup>.

**Crystal data for  $[\text{Mn}(5\text{-Brsaltmen})(\text{MeOH})_2]\text{ClO}_4 \cdot \text{MeOH}$** :  $\text{C}_{25}\text{H}_{32}\text{N}_2\text{O}_9\text{Cl}_2\text{Br}_2\text{Mn}$ ,  $M=730.71$ , monoclinic  $P2_1/n$  (no. 14),  $a=8.426(2)$ ,  $b=29.020(6)$ ,  $c=11.663(3)$  Å,  $\beta=100.499(3)^\circ$ ,  $V=2804.0(11)$  Å<sup>3</sup>,  $Z=4$ ,  $\rho_{\text{calc}}=1.731$  g cm<sup>-3</sup>,  $F_{000}=1472.00$ ,  $2\theta_{\text{max}}=62.0^\circ$ . Final  $R1=0.043$  ( $I > 2.00\sigma(I)$ ),  $R1=0.052$  (all data),  $wR2=0.134$  (all data), GOF=1.085 for 345 parameters and a total of 25655 reflections, 7930 of which were unique ( $R_{\text{int}}=0.076$ ). The linear absorption coefficient  $\mu$  for  $\text{MoK}\alpha$  radiation was 34.77 cm<sup>-1</sup>. Application of an empirical absorption correction resulted in transmission factors ranging from 0.67 to 1.00. The data were corrected for Lorentzian and polarization effects. Max. positive and negative peaks in  $\Delta F$  map were  $\rho_{\text{max}}=0.92$  e Å<sup>-3</sup> and  $\rho_{\text{min}}=-0.84$  e Å<sup>-3</sup>.

**Crystal data for  $1 \cdot 6\text{H}_2\text{O}$** :  $\text{C}_{64}\text{H}_{70}\text{N}_{10}\text{O}_{20}\text{Cl}_6\text{Mn}_2\text{Ni}$ ,  $M=1680.61$ , monoclinic  $P2_1/c$  (no. 14),  $a=16.612(4)$ ,  $b=21.467(4)$ ,  $c=20.662(4)$ ,  $\beta=102.578(4)^\circ$ ,  $V=7191.6(26)$  Å<sup>3</sup>,  $Z=4$ ,  $\rho_{\text{calc}}=1.552$  g cm<sup>-3</sup>,  $F_{000}=3456.00$ ,  $2\theta_{\text{max}}=62.4^\circ$ . Final  $R1=0.050$  ( $I > 2.00\sigma(I)$ ),  $R1=0.072$  (all data),  $wR2=0.132$  (all data), GOF=1.039 for 978 parameters and a total of 69818 reflections, 21170 of which were unique ( $R_{\text{int}}=0.054$ ). The linear absorption coefficient  $\mu$  for  $\text{MoK}\alpha$  radiation was 9.06 cm<sup>-1</sup>. Application of an empirical absorption correction resulted in transmission factors ranging from 0.93 to 1.00. The data were corrected for Lorentzian and polarization effects. Max. positive and negative peaks in  $\Delta F$  map were  $\rho_{\text{max}}=1.06$  e Å<sup>-3</sup> and  $\rho_{\text{min}}=-0.72$  e Å<sup>-3</sup>.

**Crystal and experimental data for  $2 \cdot 2\text{H}_2\text{O} \cdot \text{MeOH}$** :  $\text{C}_{65}\text{H}_{66}\text{N}_{10}\text{O}_{17}\text{Cl}_2\text{Br}_4\text{Mn}_2\text{Ni}$ ,  $M=1818.39$ , monoclinic  $P2_1/c$  (no. 14),  $a=16.732(2)$ ,  $b=21.252(4)$ ,  $c=20.756(3)$  Å,  $\beta=100.59(8)^\circ$ ,  $V=7254(1)$  Å<sup>3</sup>,  $Z=4$ ,  $\rho_{\text{calc}}=1.665$  g cm<sup>-3</sup>,  $F_{000}=3656.00$ ,  $2\theta_{\text{max}}=55.0^\circ$ . Final  $R1=0.059$  ( $I > 2.00\sigma(I)$ ),  $R1=0.114$  (all data),  $wR2=0.152$  (all data), GOF=1.005 for 909 parameters and a total of 80326 reflections, 16023 of which were unique ( $R_{\text{int}}=0.104$ ). The linear absorption coefficient  $\mu$  for  $\text{MoK}\alpha$  radiation was 29.56 cm<sup>-1</sup>. Application of an empirical absorption correction resulted in transmission factors ranging from 0.93 to 1.00. The data were corrected for Lorentzian and polarization effects. Max. positive and negative peaks in  $\Delta F$  map were  $\rho_{\text{max}}=1.44$  e Å<sup>-3</sup> and  $\rho_{\text{min}}=-0.61$  e Å<sup>-3</sup>.

CCDC-249738 ( $[\text{Mn}_2(5\text{-Brsaltmen})_2(\text{H}_2\text{O})_2](\text{ClO}_4)_2$ ), CCDC-249739 ( $[\text{Mn}(5\text{-Brsaltmen})(\text{MeOH})_2]\text{ClO}_4$ ), CCDC-249736 (**1**), and CCDC-249737 (**2**) contain the supplementary crystallographic data for this paper. These data can be obtained free of charge from The Cambridge Crystallographic Data Centre via [www.ccdc.cam.ac.uk/data\\_request/cif](http://www.ccdc.cam.ac.uk/data_request/cif).

## Acknowledgement

We thank Prof. T. Kuroda-Sowa (Kinki University) for simulating the reduced magnetization and Mr. Tomokura Madanbashi and Ms. Hitomi Takahashi (Tokyo Metropolitan University) for help in X-ray crystallographic analyses. H.M. is grateful for financial support from the PRESTO project, Japan Science and Technology Agency (JST), and a

Grant-in-Aid for Scientific Research from the Ministry of Education, Culture, Sports, Science, and Technology, Japan. M.Y. is grateful for financial support from the CREST project of JST. R.C. thanks the CNRS, the University of Bordeaux 1, and the Conseil Regional d'Aquitaine for financial support.

- [1] Reviews: G. Christou, D. Gatteschi, D. N. Hendrickson, R. Sessoli, *MRS Bull.* **2000**, 25, 66; D. Gatteschi, R. Sessoli, *Angew. Chem.* **2003**, 115, 278; *Angew. Chem. Int. Ed.* **2003**, 42, 268–297.
- [2] a) P. D. W. Boyd, Q. Li, J. B. Vincent, K. Folting, H. -R. Chang, W. E. Streib, J. C. Huffman, G. Christou, D. N. Hendrickson, *J. Am. Chem. Soc.* **1988**, 110, 8537; b) A. Caneschi, D. Gatteschi, R. Sessoli, *J. Am. Chem. Soc.* **1991**, 113, 5873; c) R. Sessoli, H.-L. Tsai, A. R. Schake, S. Wang, J. B. Vincent, K. Folting, D. Gatteschi, G. Christou, D. N. Hendrickson, *J. Am. Chem. Soc.* **1993**, 115, 1804.
- [3] Mn<sub>12</sub> derivatives: a) H. J. Eppley, H.-L. Tsai, N. de Vries, K. Folting, G. Christou, D. N. Hendrickson, *J. Am. Chem. Soc.* **1995**, 117, 301; b) S. M. J. Aubin, Z. Sun, L. Pardi, J. Krzystek, K. Folting, L.-C. Brunel, A. L. Rheingold, G. Christou, D. N. Hendrickson, *Inorg. Chem.* **1999**, 38, 5329; c) M. Soler, S. K. Chandra, D. Ruiz, E. R. Davidson, D. N. Hendrickson, G. Christou, *Chem. Commun.* **2000**, 2417; d) H.-L. Tsai, T.-Y. Jwo, G.-H. Lee, Y. Wang, *Chem. Lett.* **2000**, 346; e) S. M. J. Aubin, Z. Sun, H. J. Eppley, E. M. Rumberger, I. A. Guzei, K. Folting, P. K. Gantzel, A. L. Rheingold, G. Christou, D. N. Hendrickson, *Inorg. Chem.* **2001**, 40, 2127; f) T. Kuroda-Sowa, M. Lam, A. L. Rheingold, C. Frommen, W. M. Reiff, M. Nakano, J. Yoo, A. L. Maniero, L.-C. Brunel, G. Christou, D. N. Hendrickson, *Inorg. Chem.* **2001**, 40, 6469; g) D. N. Hendrickson, G. Christou, H. Ishimoto, J. Yoo, E. K. Brechin, A. Yamaguchi, E. M. Rumberger, S. M. J. Aubin, Z. Sun, G. Aromi, *Polyhedron* **2001**, 20, 1479; h) C.-D. Park, S. W. Rhee, Y. Kim, W. Jeon, D.-Y. Jung, D.-H. Kim, Y. Do, H.-C. Ri, *Bull. Korean Chem. Soc.* **2001**, 22, 453; i) A. Forment-Aliaga, E. Coronado, M. Feliz, A. Gaita-Arino, R. Llusar, F. M. Romero, *Inorg. Chem.* **2003**, 42, 8019; j) M. Soler, W. Wernsdorfer, Z. Sun, J. C. Huffman, D. N. Hendrickson, G. Christou, *Chem. Commun.* **2003**, 2672; k) N. E. Chakov, W. Wernsdorfer, K. A. Abboud, D. N. Hendrickson, G. Christou, *J. Chem. Soc. Dalton Trans.* **2003**, 2243; l) M. Soler, W. Wernsdorfer, K. A. Abboud, J. C. Huffman, E. R. Davidson, D. N. Hendrickson, G. Christou, *J. Am. Chem. Soc.* **2003**, 125, 3576; m) T. Kuroda-Sowa, T. Nogami, H. Konaka, M. Maekawa, M. Munakata, H. Miyasaka, M. Yamashita, *Polyhedron* **2003**, 22, 1795–1801; n) H. Zhao, C. P. Berlinguette, J. Bacsa, A. V. Prosvirin, J. K. Bera, S. E. Tichy, E. J. Schelter, K. R. Dunbar, *Inorg. Chem.* **2004**, 43, 1359; o) G.-Q. Bian, T. Kuroda-Sowa, H. Konaka, M. Hatano, M. Maekawa, M. Munakata, H. Miyasaka, M. Yamashita, *Inorg. Chem.* **2004**, 43, 4790.
- [4] Mn SMMs: a) S. M. J. Aubin, M. W. Wemple, D. M. Adams, H. Tsai, G. Christou, D. N. Hendrickson, *J. Am. Chem. Soc.* **1996**, 118, 7746; b) J. Yoo, E. K. Brechin, A. Yamaguchi, M. Nakano, J. C. Huffman, A. L. Maniero, L.-C. Brunel, K. Awaga, H. Ishimoto, G. Christou, D. N. Hendrickson, *Inorg. Chem.* **2000**, 39, 3615; c) J. Yoo, A. Yamaguchi, M. Nakano, J. Krzystek, W. E. Streib, L.-C. Brunel, H. Ishimoto, G. Christou, D. N. Hendrickson, *Inorg. Chem.* **2001**, 40, 4604; d) C. Boskovic, E. K. Brechin, W. E. Streib, K. Folting, D. N. Hendrickson, G. Christou, *J. Am. Chem. Soc.* **2002**, 124, 3725; e) E. K. Brechin, C. Boskovic, W. Wernsdorfer, J. Yoo, A. Yamaguchi, E. C. Sanudo, T. Concolino, A. L. Rheingold, H. Ishimoto, D. N. Hendrickson, G. Christou, *J. Am. Chem. Soc.* **2002**, 124, 9710; f) E. K. Brechin, M. Soler, J. Davidson, D. N. Hendrickson, S. Parsons, G. Christou, *Chem. Commun.* **2002**, 2252; g) C. Boskovic, R. Bircher, P. L. W. Tregenna-Piggott, H. U. Güdel, C. Paulsen, W. Wernsdorfer, A.-L. Barra, E. Khatsko, A. Neels, H. Stoeckli-Evans, *J. Am. Chem. Soc.* **2003**, 125, 14046; h) H. Miyasaka, R. Clérac, W. Wernsdorfer, L. Lecren, C. Bonhomme, K. Sugiura, M. Yamashita, *Angew. Chem.* **2004**, 116, 2861; *Angew. Chem. Int. Ed.* **2004**, 43, 2801; i) A. J. Tasio-poulos, A. Vinslava, W. Wernsdorfer, K. A. Abboud, G. Christou, *Angew. Chem.* **2004**, 116, 2169; *Angew. Chem. Int. Ed.* **2004**, 43, 2117; j) M. Murugesu, M. Habrych, W. Wernsdorfer, K. A. Abboud, G. Christou, *J. Am. Chem. Soc.* **2004**, 126, 4766; k) M. Soler, W. Wernsdorfer, K. Folting, M. Pink, G. Christou, *J. Am. Chem. Soc.* **2004**, 126, 2156; l) M. Murugesu, J. Raftery, W. Wernsdorfer, G. Christou, E. Brechin, *Inorg. Chem.* **2004**, 43, 4203; m) E. C. Sanudo, W. Wernsdorfer, K. A. Abboud, G. Christou, *Inorg. Chem.* **2004**, 43, 4137; n) L. M. Wittick, K. S. Murray, B. Moubaraki, S. R. Batten, L. Spiccia, K. Berry, *Dalton Trans.* **2004**, 1003; o) N. Aliaga-Alcalde, R. S. Edwards, S. O. Hill, W. Wernsdorfer, K. Folting, G. Christou, *J. Am. Chem. Soc.* **2004**, 126, 12503.
- [5] Fe SMMs: a) C. Delfs, D. Gatteschi, L. Pardi, R. Sessoli, K. Wieghardt, D. Hanke, *Inorg. Chem.* **1993**, 32, 3099; b) A. L. Barra, A. Caneschi, A. Cornia, F. Fabrizi de Biani, D. Gatteschi, C. Sangregorio, R. Sessoli, L. Sorace, *J. Am. Chem. Soc.* **1999**, 121, 5302; c) D. Gatteschi, R. Sessoli, A. Cornia, *Chem. Commun.* **2000**, 725; d) H. Oshio, N. Hoshino, T. Ito, *J. Am. Chem. Soc.* **2000**, 122, 12602; e) C. Benelli, J. Cano, Y. Journaux, R. Sessoli, G. A. Solan, R. E. P. Winpenny, *Inorg. Chem.* **2001**, 40, 188; f) J. C. Goodwin, R. Sessoli, D. Gatteschi, W. Wernsdorfer, A. K. Powell, S. L. Heath, *J. Chem. Soc. Dalton Trans.* **2000**, 1835; g) H. Oshio, N. Hoshino, T. Ito, M. Nakano, *J. Am. Chem. Soc.* **2004**, 126, 8805.
- [6] Ni SMMs: a) C. Cadiou, M. Murrice, C. Paulsen, V. Villar, W. Wernsdorfer, R. E. P. Winpenny, *Chem. Commun.* **2001**, 2666; b) H. Andres, R. Basler, A. J. Blake, C. Cadiou, G. Chaboussant, C. M. Grant, H.-U. Güdel, M. Murrice, S. Parsons, C. Paulsen, F. Semadini, V. Villar, W. Wernsdorfer, R. E. P. Winpenny, *Chem. Eur. J.* **2002**, 8, 4867; c) E.-C. Yang, W. Wernsdorfer, S. Hill, R. S. Edwards, M. Nakano, S. Maccagnano, L. N. Zakharov, A. L. Rheingold, G. Christou, D. N. Hendrickson, *Polyhedron* **2003**, 22, 1727; d) M. Moragues-Cánovas, M. Helliwell, L. Ricard, É. Rivière, W. Wernsdorfer, E. Brechin, T. Mallah, *Eur. J. Inorg. Chem.* **2004**, 2219.
- [7] V SMMs: S. L. Castro, Z. Sun, C. M. Grant, J. C. Bollinger, D. N. Hendrickson, G. Christou, *J. Am. Chem. Soc.* **1998**, 120, 2365.
- [8] Co SMMs: E. Yang, D. N. Hendrickson, W. Wernsdorfer, M. Nakano, L. N. Zakharov, R. D. Sommer, A. L. Rheingold, M. Ledezma-Gairaud, G. Christou, *J. Appl. Phys.* **2002**, 91, 7382.
- [9] Mixed-metal SMMs: a) A. R. Schake, H. Tsai, R. J. Webb, K. Folting, G. Christou, D. N. Hendrickson, *Inorg. Chem.* **1994**, 33, 6020; b) J. J. Sokol, A. G. Hee, J. R. Long, *J. Am. Chem. Soc.* **2002**, 124, 7656; c) S. Karasawa, G. Zhou, H. Morikawa, N. Koga, *J. Am. Chem. Soc.* **2003**, 125, 13676; d) H. J. Choi, J. J. Sokol, J. R. Long, *Inorg. Chem.* **2004**, 43, 1606; e) S. Osa, T. Kido, N. Matsumoto, N. Re, A. Pochaba, J. Mrozinski, *J. Am. Chem. Soc.* **2004**, 126, 420; f) C. M. Zaleski, E. C. Deppner, J. W. Kampf, M. L. Kirk, V. L. Pecoraro, *Angew. Chem.* **2004**, 116, 4002; *Angew. Chem. Int. Ed.* **2004**, 43, 3912.
- [10] a) A. Caneschi, D. Gatteschi, N. Lalioti, C. Sangregorio, R. Sessoli, G. Venturi, A. Vindigni, A. Rettori, M. G. Pini, M. A. Novak, *Angew. Chem.* **2001**, 113, 1810; *Angew. Chem. Int. Ed.* **2001**, 40, 1760; b) A. Caneschi, D. Gatteschi, N. Lalioti, C. Sangregorio, R. Sessoli, G. Venturi, A. Vindigni, A. Rettori, M. G. Pini, M. A. Novak, *Europhys. Lett.* **2002**, 58, 771; c) L. Bogani, A. Caneschi, M. Fedi, D. Gatteschi, M. Massi, M. A. Novak, M. G. Pini, A. Rettori, R. Sessoli, A. Vindigni, *Phys. Rev. Lett.* **2004**, 92, 20, 207204-1; d) L. Bogani, A. Caneschi, M. Fedi, D. Gatteschi, M. Massi, M. A. Novak, M. G. Pini, A. Rettori, R. Sessoli, A. Vindigni, *Phys. Rev. Lett.* **2004**, 92, 20, 207204–207201.
- [11] a) R. Clérac, H. Miyasaka, M. Yamashita, C. Coulon, *J. Am. Chem. Soc.* **2002**, 124, 12837; b) H. Miyasaka, R. Clérac, K. Mizushima, K. Sugiura, M. Yamashita, W. Wernsdorfer, C. Coulon, *Inorg. Chem.* **2003**, 42, 8203; c) C. Coulon, R. Clérac, L. Lecren, W. Wernsdorfer, H. Miyasaka, *Phys. Rev. B* **2004**, 69, 132408.
- [12] a) R. Lescouëzec, J. Vaissermann, C. Ruiz-Pérez, F. Lloret, R. Carasco, M. Julve, M. Verdaguer, Y. Dromzee, D. Gatteschi, W. Wernsdorfer, *Angew. Chem.* **2003**, 115, 1521; *Angew. Chem. Int. Ed.* **2003**, 42, 1483; b) L. M. Toma, R. Lescouëzec, F. Lloret, M. Julve, J. Vaissermann, M. Verdaguer, *Chem. Commun.* **2003**, 1850.
- [13] a) T. Liu, D. Fu, S. Gao, Y. Zhang, H. Sun, G. Su, Y. Liu, *J. Am. Chem. Soc.* **2003**, 125, 13976; b) N. Shaikh, A. Panja, S. Goswami, P. Banerjee, P. Vojtyšek, Y.-Z. Zhang, G. Su, S. Gao, *Inorg. Chem.*

- 2004, 43, 849; c) S. Wang, J.-L. Zuo, S. Gao, Y. Song, H.-C. Zhou, Y.-Z. Zhang, X.-Z. You, *J. Am. Chem. Soc.* **2004**, 126, 8900; d) N. E. Chakov, W. Wernsdorfer, K. A. Abboud, G. Christou, *Inorg. Chem.* **2004**, 43, 5919; e) E. Pardo, R. Ruiz-Garcia, F. Lloret, J. Faus, M. Julve, Y. Journaux, F. Delgado, C. Ruiz-Perez, *Adv. Mater.* **2004**, 16, 18, 1597.
- [14] a) R. J. Glauber, *J. Math. Phys.* **1963**, 4, 294; b) M. Susuki, R. Kubo, *J. Phys. Soc. Japan* **1968**, 24, 51.
- [15] H. Miyasaka, R. Clérac, T. Ishii, H.-C. Chang, S. Kitagawa, M. Yamashita, *J. Chem. Soc. Dalton Trans.* **2002**, 1528.
- [16] H. Miyasaka, S. Furukawa, S. Yanagida, K. Sugiura, M. Yamashita, *Inorg. Chim. Acta* **2004**, 357, 1619.
- [17] H. Miyasaka, R. Clérac, unpublished results.
- [18] B. E. Myers, L. Berger, S. Friedberg, *J. Appl. Phys.* **1969**, 40, 1149; C. J. O'Connor, *Prog. Inorg. Chem.* **1982**, 29, 203.
- [19] H. Miyasaka, T. Nezu, K. Sugimoto, K. Sugiura, M. Yamashita, R. Clérac, *Inorg. Chem.* **2004**, 43, 5486.
- [20] Based on  $J$  values, the  $S_T=3$  spin ground state can be considered to be the only populated state below 10 K. This can be intuitively seen in Figure 6 and in the fitting curve for the model with isolated trinuclear units (blue line in Figure 4). The  $\chi T$  product reaches a plateau below 10 K at the corresponding value for the  $S_T=3$  state.
- [21] a) M. Matsuura, Y. Okuda, M. Morotomi, H. Mollmoto, M. Date, *J. Phys. Soc. Jpn.* **1979**, 46, 1031; b) H. Miyasaka, K. Nakata, K. Sugiura, M. Yamashita, R. Clérac, *Angew. Chem.* **2004**, 116, 725; *Angew. Chem. Int. Ed.* **2004**, 43, 707; c) P. King, R. Clérac, W. Wernsdorfer, C. E. Anson, A. K. Powell, *Dalton Trans.* **2004**, 2670.
- [22] The well-known expression  $2zJ^2S_T^2 = gS_T\mu_B H_{ex}$  was used A. Herpin, "Théorie du magnétisme", *Bibl. des Sciences et Techn. Nucl.*, Presses Univ. de France, **1968**.
- [23] The measurements were performed on a polycrystalline sample, and therefore all directions are simultaneously explored by the applied field.
- [24] Minimization of the anisotropy and Zeeman energies gives  $2DS^2 \approx g\mu_B SH_a$ ; B. Barbara, L. Thomas, F. Lioni, I. Chiorescu, A. Sulpice, *J. Magn. Magn. Mater.* **1999**, 200, 167.
- [25] E. A. Boudreaux, L. N. Mulay, *Theory and Applications of Molecular Paramagnetism*, Wiley, New York **1976**.
- [26] A. Altomare, M. Burla, M. Camalli, G. Cascarano, C. Giacovazzo, A. Guagliardi, A. Moliterni, G. Polidori, R. Spagna, *J. Appl. Crystallogr.* **1999**, 32, 115.
- [27] P. T. Beurskens, G. Admiraal, G. Beurskens, W. P. Bosman, R. de Gelder, R. Israel, J. M. M. Smits, The DIRDIF-99 program system, Technical Report of the Crystallography Laboratory, University of Nijmegen, The Netherlands, **1999**.
- [28] D. T. Cromer, J. T. Waber, *International Tables for Crystallography, Vol. IV*, The Kynoch Press, **1974**, Table 2.2A.
- [29] D. C. Creagh, W. J. McAuley, *International Tables for Crystallography, Vol. C* (Ed.: A. J. C. Wilson), Kluwer Academic Publishers, Boston, **1992**, Table 4.2.6.8, pp. 219–222.
- [30] D. C. Creagh, J. H. Hubbell, *International Tables for Crystallography, Vol. C*, (Ed.: A. J. C. Wilson), Kluwer Academic Publishers, Boston, **1992**, Table 4.2.4.3, pp. 200–206.
- [31] CrystalStructure 3.15: crystal structure analysis package, Rigaku and Rigaku/MS (2000–2002), 9009 New Trails Dr., The Woodlands TX 77381, USA.

Received: September 16, 2004  
Published online: January 20, 2005